



**HAL**  
open science

# A co-simulation approach to study the impact of gravity collective irrigation constraints on plant dynamics in Southern France

Bastien Richard, Bruno Bonté, Magalie Delmas, Isabelle Braud, Bruno Cheviron, Julien Veyssier, Olivier Barreteau

## ► To cite this version:

Bastien Richard, Bruno Bonté, Magalie Delmas, Isabelle Braud, Bruno Cheviron, et al.. A co-simulation approach to study the impact of gravity collective irrigation constraints on plant dynamics in Southern France. *Agricultural Water Management*, 2022, 262, pp.107205. 10.1016/j.agwat.2021.107205 . hal-03522515

**HAL Id: hal-03522515**

**<https://hal.inrae.fr/hal-03522515>**

Submitted on 8 Jan 2024

**HAL** is a multi-disciplinary open access archive for the deposit and dissemination of scientific research documents, whether they are published or not. The documents may come from teaching and research institutions in France or abroad, or from public or private research centers.

L'archive ouverte pluridisciplinaire **HAL**, est destinée au dépôt et à la diffusion de documents scientifiques de niveau recherche, publiés ou non, émanant des établissements d'enseignement et de recherche français ou étrangers, des laboratoires publics ou privés.



Distributed under a Creative Commons Attribution - NonCommercial 4.0 International License

# 1 **A co-simulation approach to study the impact of gravity collective irrigation constraints on** 2 **plant dynamics in Southern France**

3 Bastien Richard<sup>a,b</sup>, Bruno Bonté<sup>a</sup>, Magalie Delmas<sup>a</sup>, Isabelle Braud<sup>b</sup>, Bruno Cheviron<sup>a</sup>, Julien  
4 Veyssier<sup>a,b</sup>, Olivier Barreteau<sup>a</sup>

5 <sup>a</sup> G-EAU, Univ Montpellier, AgroParisTech, CIRAD, IRD, INRAE, Montpellier SupAgro, Montpellier,  
6 France.

7 <sup>b</sup> INRAE, RiverLy, 69100, Villeurbanne, France.

8 The corresponding author for all stages of refereeing and publication, also post-publication: Bastien  
9 Richard, +33 6 74 93 64 42, [bastien.richard@inrae.fr](mailto:bastien.richard@inrae.fr), 361 Rue Jean François Breton, 34196  
10 Montpellier, France.

## 11 **Abstract**

12 Crop models allow simulating irrigated plant dynamics at the plot level. However, in many places  
13 irrigation is managed collectively to share water at the network level. To study the impact of the  
14 irrigation network constraints on plant dynamics, we proposed a co-simulation approach based on  
15 the coupling of the Optirrig crop model at the plot level with the WatASit agent-based model at the  
16 network level. As a proof of concept applied on a typical gravity network of the South-East of France,  
17 the approach allowed to consider the effects of the network spatial (i.e. water flow gradient) and  
18 temporal (i.e. network coordination) constraints on leaf area index and water stress index dynamics  
19 of 16 cereal plots. Four progressive levels of collective irrigation constraints are simulated: no  
20 collective constraints, space collective constraints, time collective constraints, and space and time  
21 collective constraints. Retrospective simulation of the 2017 irrigation campaign is consistent with  
22 field surveys, and simulation results suggest that plant water stress could be underestimated when  
23 simulated at the plot level rather than at the network level. Spatially, the most severe water stress  
24 was observed for the plants located furthest downstream of the network. Temporally, the absence of  
25 network coordination can lead to earlier plant water stress and lower plant growth during the  
26 collective irrigation campaign, while time-slot-based coordination tends to delay the impact. For  
27 future research, reinforcing the coupling from the crop model to the agent-based model could allow  
28 to study the feedback loop of plant dynamics on irrigation practice adaptations. It is also a first step  
29 towards an optimization approach for irrigation networks.

30 **Keywords:** co-simulation; irrigation network; crop model; agent-based model; water stress; WSI;  
31 LAI.

## 32 **1. Introduction**

33 Crop models simulate plant dynamics according to the climate-soil-plant interactions.  
34 Therefore, they are useful to evaluate the effects of irrigation on plant growth and water stress at the  
35 plot level. In recent years, several simulation platforms (e.g. RECORD, HarvestChoice; MAELIA)  
36 have been developed firstly to facilitate the automation of crop models, but also to better take into

37 account context-dependent constraints at other levels than the plot level (HarvestChoice, 2010;  
38 Gaudou et al., 2013).

39 On the other hand, agent-based models (ABMs) have been widely used within the last few  
40 years to study systems involving complex interactions between human actions and their biophysical  
41 and/or social environment. They offer possibilities for incorporating disparate entities and for studying  
42 their local interactions (Bousquet and le Page, 2004; Matthews et al., 2007). They are well suited to  
43 take into consideration key micro-level constraints rather than aggregated system representations  
44 (Filatova et al., 2013), especially the agriculture-environment interactions (e.g. Valbuena et al.,  
45 2010).

46 Scholars have explored various ways for associating agent-based models (ABMs) with crop  
47 models for two decades, leading to modeling and simulation environments embedding biophysical,  
48 economic, or socioeconomic components (Berntsen et al., 2003; Belcher et al., 2004). AquaCrop  
49 (Raes et al., 2009; Steduto et al., 2009) was combined with an economic model (García-Vila and  
50 Fereres, 2012). STICS (Brisson et al., 2003) was implemented in the RECORD platform to represent  
51 farming practices into agro-ecosystems. APSIM (McCown et al., 1995; Keating et al., 2003) or  
52 DSSAT (Jones et al., 2003) have been embedded in the HarvestChoice (2010) platform to nourish  
53 regional-scale decision-making. WOFO5 (Wolf and van Diepen, 1995; Reidsma et al., 2009; Supit  
54 et al., 2012) was reformulated into the modular Python Crop Simulation Development programming  
55 structure (de Wit, 2015). Gaudou et al. (2013) have integrated AqYield (Nolot and Debaeke, 2003;  
56 Murgue et al., 2014; Constantin et al., 2015) into the MAELIA multi-agent platform.

57 Several studies have shown the usefulness of coupling cellular components representing a  
58 landscape with an agent-based simulator at the household or farmer level with behaviors that alter  
59 the landscape (Parker et al., 2003; Verburg et al., 2004; Berger et al., 2006). Such approaches  
60 enable assessing the environmental, economic, and social impacts of the combined changes in  
61 agricultural activities (demography, dynamics of land cover and climate). Thanks to these platforms,  
62 changes in cropping systems, access to water, irrigation inputs cost and availability, have been  
63 assessed in terms of their impact on plant dynamics, notably through proxies of plant development  
64 and production such as the *Leaf Area Index (LAI)* (Monteith, 1977) and the *Water Stress Index (WSI)*  
65 (Jones, 1992).

66 However, few scholars have proposed to study the potential impacts due to irrigation network  
67 constraints on plant dynamics. In particular, in gravity-fed networks, Merot et al. (2008) have shown  
68 the importance of water distribution constraints and irrigation inter-related practices to ensure  
69 irrigation operations in the Crau plain (France). At the level of the irrigated scheme, the spatial  
70 constraints to operate irrigation include, for example, the variation of flow rate and water availability  
71 along the upstream-downstream gradient in the abduction network, according to its withdrawals,  
72 seepage, and hydraulic limitations. During the irrigation campaign, the possibilities for temporal  
73 adjustment of irrigators' calendar are thus limited by these spatial constraints and depend on the

74 behavior of other irrigators influencing the network flow rate. In particular, irrigation coordination is a  
75 key factor for sharing water resource that must be distributed through a common network in the right  
76 place and time to all along the irrigation campaign. In this context, our simulation approach aims at  
77 capturing the potential impacts of spatial (i.e. network flow gradient) and temporal (i.e. network  
78 coordination) constraints due to a gravity irrigation network on plant LAI and WSI dynamics.

79 Integrated simulation approaches that merge models into a unified software package (e.g.  
80 Matthews, 2006; Schreinemachers et al., 2007; Gaudou et al., 2013) are useful to capture the  
81 complex human-environment interactions and shed light on the understanding of the system  
82 dynamics with potential entry-points for policy design (Dragan et al., 2003). However, model  
83 simplifications commonly occur when merging modules, especially of environmental processes (e.g.  
84 Schreinemachers et al., 2007, 2010), altering the model's ability to fully capture interactions. A more  
85 flexible method called co-simulation, also used by scholars in farming and environmental modeling  
86 (e.g. Warner et al., 2008; Bithell and Brasington, 2009; Bulatewicz et al., 2010), consist in coupling  
87 simulation software together rather than integrating individual components in a single modeling and  
88 simulation software. The main advantage is that there is no need for recoding components and  
89 consequently the users and developer's community of each model component may be asked to help  
90 with the coupled model (control code, provide and test new modules, ...). However, it involves  
91 conceptual and programming developments to ensure compatibility of many characteristics including  
92 basic assumptions, spatial and time scales. First, it requires to make sure that models components  
93 and associated software have communication features and manage disruption correctly. Last but not  
94 least, it requires a clear conceptual approach to organize scheduling between the models and  
95 between the simulation software.

96 The objective of this paper is to present a co-simulation approach based on the coupling of  
97 the Optirrig crop model at the plot level with the WatASit agent-based model at the irrigation network  
98 level. As a proof of concept, we applied the approach for capturing the potential impact of a typical  
99 gravity-fed network in the South-East of France on 16 cereal plots. We simulated a dry year irrigation  
100 campaign under four levels of collective irrigation constraints (i.e. no collective constraint, space  
101 collective constraint, time collective constraint, and space and time collective constraints), and we  
102 compared LAI and WSI dynamics of cereal plots.

103 The next sections present the overall co-simulation approach (Section 2), the study area and  
104 the specific models developed for the proof of concept (Section 3), and the simulation results for the  
105 four levels of collective irrigation constraints (Section 4), before discussing the added-value,  
106 limitations and perspectives in Section 5.

## 107 **2. Singular features of the co-simulation approach**

### 108 2.1 Overview

109 The purpose of the co-simulation is to capture the potential impacts on crop LAI and WSI  
110 dynamics induced by the gravity irrigation network when operating irrigation during a collective  
111 irrigation campaign. The approach consists in linking a crop model at the plot level, and an ABM at  
112 the network level, based on the daily coupling of their two simulation software described in Table 1.  
113 It uses the Optirrig crop model for simulating *LAI* and *WSI* as a proxy for crop development and water  
114 stress, and the WatASit ABM at the network level for generating irrigation operations under four  
115 progressive levels of collective irrigation constraints (see Section 3.6). Optirrig simulates climate-  
116 soil-plant interactions daily in which irrigation dates (*I+*) on each plot are forced by WatASit through  
117 a daily coupling (Fig. 1). WatASit is itself nourished by the state of maturity of the crops (*TT*) provided  
118 by the Optirrig model. If there is a conflict for the sharing of water in the collective gravity network, it  
119 is managed by the ABM and may induce a delay in irrigation for some of the irrigators who would  
120 aim to irrigate at the same time.

121 **Table 1.** Main characteristics of Optirrig and WatASit models and simulation software.

Characteristic	Optirrig	WatASit
Scientific domain	Irrigation optimization, plant production, soil science	Operational management of collective irrigation, coordination
Type of model	Process-based crop model	Agent-based model of irrigation operations under space and time collective constraints
Main assumptions	- The time-evolution of crop water stress quantified by <i>WSI</i> values is the main control over <i>LAI</i> values, with dedicated effects associated with the severity and time of occurrence of water stresses, and this time-evolution is the consequence of both rain and irrigation events	- Priority is given to the plot that has not been irrigated for the longest time - A maximum irrigation operations at a time per irrigator - Number of irrigators per farm is taken into account
Components	- Soil water balance - Plant growth - Total dry matter and agricultural yield - Crop water stress	- Irrigation possibilities simulator - Decision-making (irrigation strategy under collective constraints)
Internal processes	- Soil water reservoirs dynamics - Biomass growth - Crop management options	- Multi-scale irrigation constraints - Network flow - Network coordination options
Inputs and parameters	- Climate inputs - Land cover inputs - Soils parameters	- Climate inputs - Land cover inputs - Network parameters
Temporal resolution	Daily time step	Hourly and daily time steps
Spatial resolution	1D with no explicit representation of domain size. The nominal scale is plot-scale with possible adaptations by assuming "homogeneous" domains of any size and performing "1D multi-local" runs for down-scaling or up-scaling	Grid-cell based ; size and number of pixel user defined
Simulation platform	R (R Core Team, 2018)	CORMAS (Bommel et al., 2015)

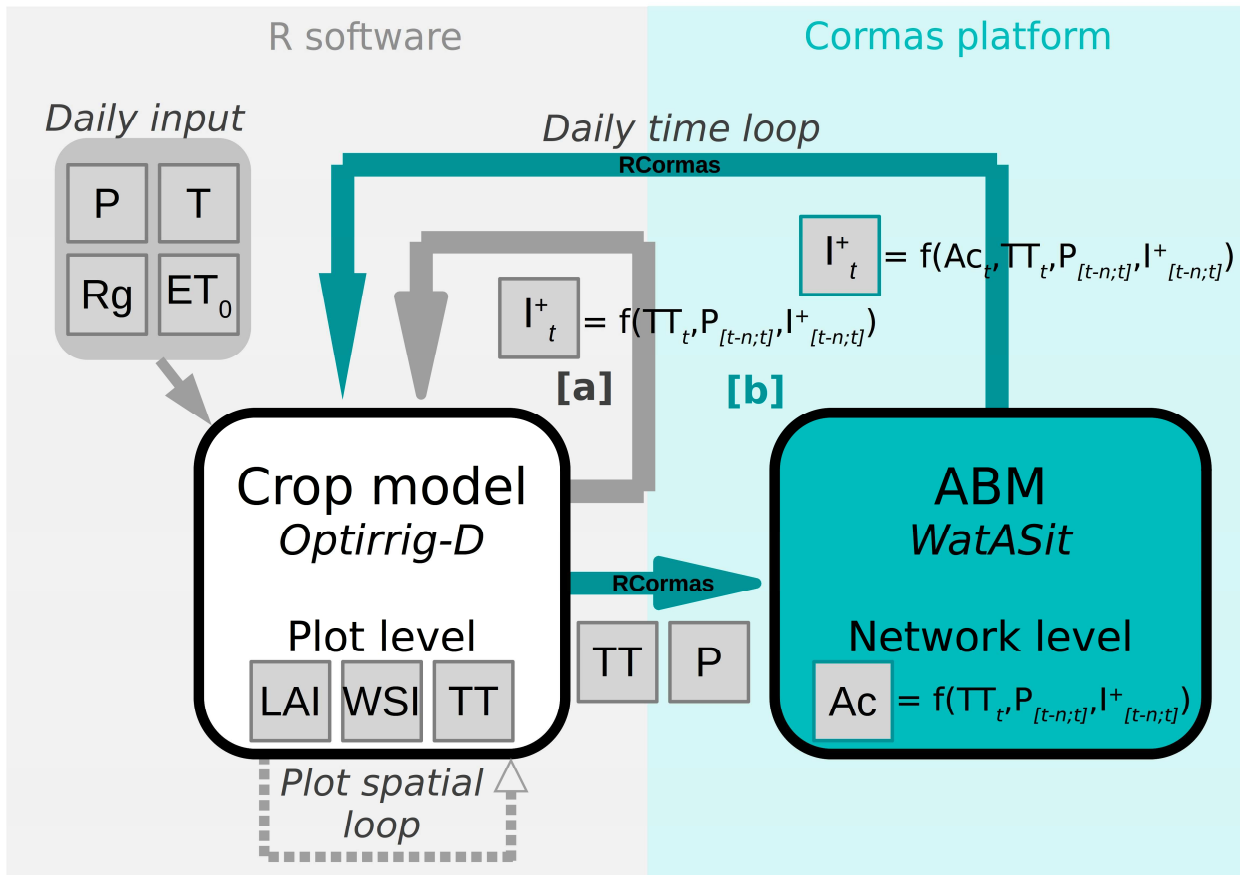


Fig. 1 (to be printed in color): Scheme of the co-simulation approach. [a] indicates the simulation processes which shortcuts the coupling with the ABM (grey arrows), whose grey boxes are the main variables. The precipitation, temperature, global radiation, and reference evapotranspiration are denoted P, T, Rg, and ET<sub>0</sub>, respectively. LAI is the Leaf Area Index, WSI the Water Stress Index and TT the sum of temperature. I<sup>+</sup> stands for irrigation, which is denoted with a "+" to indicate it depends on the irrigation decision rules. t is the current time step, whereas [t-n;t] is the time period of the last n days. [b] indicates the simulation chain which integrates the coupling with the ABM at the network level (blue arrows). In this case, I<sup>+</sup> also depends on the actions (Ac) carried out by the agents. RCormas refers to the API used for activation of the coupling and communication between the R software and the CORMAS platform.

122

123 2.2 Technical features

124 Co-simulation involves the communication of several model components that include their  
 125 solvers (meaning that the components can compute of the effects of external events and time  
 126 advance). These components are viewed as slaves' processes and are orchestrated by an external  
 127 program referred to as a master algorithm.

128 The co-simulation approach has required then the development of specifics *Application*  
 129 *Programming Interface* (APIs) designed as sets of R functions, so that the model components that

130 we used can be driven as slave processes by the master algorithm. The first API called *RCormas*<sup>1</sup>,  
131 is based on the HTTP protocol and allows communication between the R software in which the  
132 master algorithm is implemented and the CORMAS platform running the ABM. We will call the  
133 second API the Roptirrig that enable the master algorithm to communicate with the Optirrig-D  
134 simulator already coded in R. Both APIs allow piloting the simulations by initializing the model, getting  
135 and setting values from entities, and running simulation steps.

136 The master algorithm uses those APIs to first initialize both models and then to run two  
137 phases of simulation that are organized as follows:

138 [a] In the time period from the beginning of the simulation to the beginning of the irrigation campaign,  
139 no irrigation is present and the crop-related *LAI*, *WSI*, and *TT* variables are calculated by the crop  
140 model from the climatic forcing only (Fig. 1 [a]),

141 [b] During the irrigation campaign, the coupling between the crop model at the plot level and the  
142 ABM at the network level is activated. The crop model (Optirrig-D) keeps the history of all necessary  
143 state variables from one day to another and calculates the state variables according to the daily  
144 update of *I+* transmitted by the ABM on each plot (Fig. 1 [b]). Each day, first the crop model simulates  
145 *LAI*, *WSI*, and *TT* for each crop. We assume that the crop growth process is slow enough that we do  
146 not need to calculate it by the hour. The precipitation *P* and the sum of temperature *TT* are then  
147 transmitted to the ABM. Second, the ABM generates the irrigation operations made by the agents  
148 constrained by the collective network that could modify *I+* for the current day. Third, *I+* is collected  
149 and transferred to the crop model for each plot, and new *LAI* and *WSI* are computed. This sequence  
150 is repeated every day until the end of the simulation period.

151 In both [a] and [b], if *TT* exceeds the cereal temperature of maturity *TM*, the irrigation  
152 campaign is stopped for the cereal plot (*I+* is null). In the end, the original features of the approach  
153 are the consideration of a collective level of spatial and temporal constraints to operate irrigation,  
154 simulated within the gravity network thanks to the ABM, and their daily consequences for the  
155 dynamics of plants *LAI* and *WSI* at the plot level.

### 156 **3. Study area and specific models developed for the proof of concept**

#### 157 3.1 Study area and data collection

158 To illustrate the co-simulation approach, we selected the Aspres-Sur-Buëch case study (Fig.  
159 2), in which 83 plots can be irrigated by 10 irrigators sharing the gravity-fed network. The case study  
160 is located in the Buëch catchment, a sub-basin of the Durance with a surface area of 1490 km<sup>2</sup> in  
161 France. Collective irrigation constitutes by far the use that takes the most from the water resource  
162 during the low water period from May to October. Several irrigator unions are equipped either for  
163 gravity-fed irrigation, or for pressurized irrigation, or both (Fig. 2, right-side). The Aspres-sur-Buëch

1 <sup>1</sup> RCormas is available at <https://gitlab.irstea.fr/cormas-dev/r-cormas>.

164 gravity network is fairly representative in terms of location (in the upstream part of the basin), irrigable  
 165 area (with 75 ha whereas the average is 50 ha in 2017), and crop rotation (23.7% cereals in 2017).  
 166

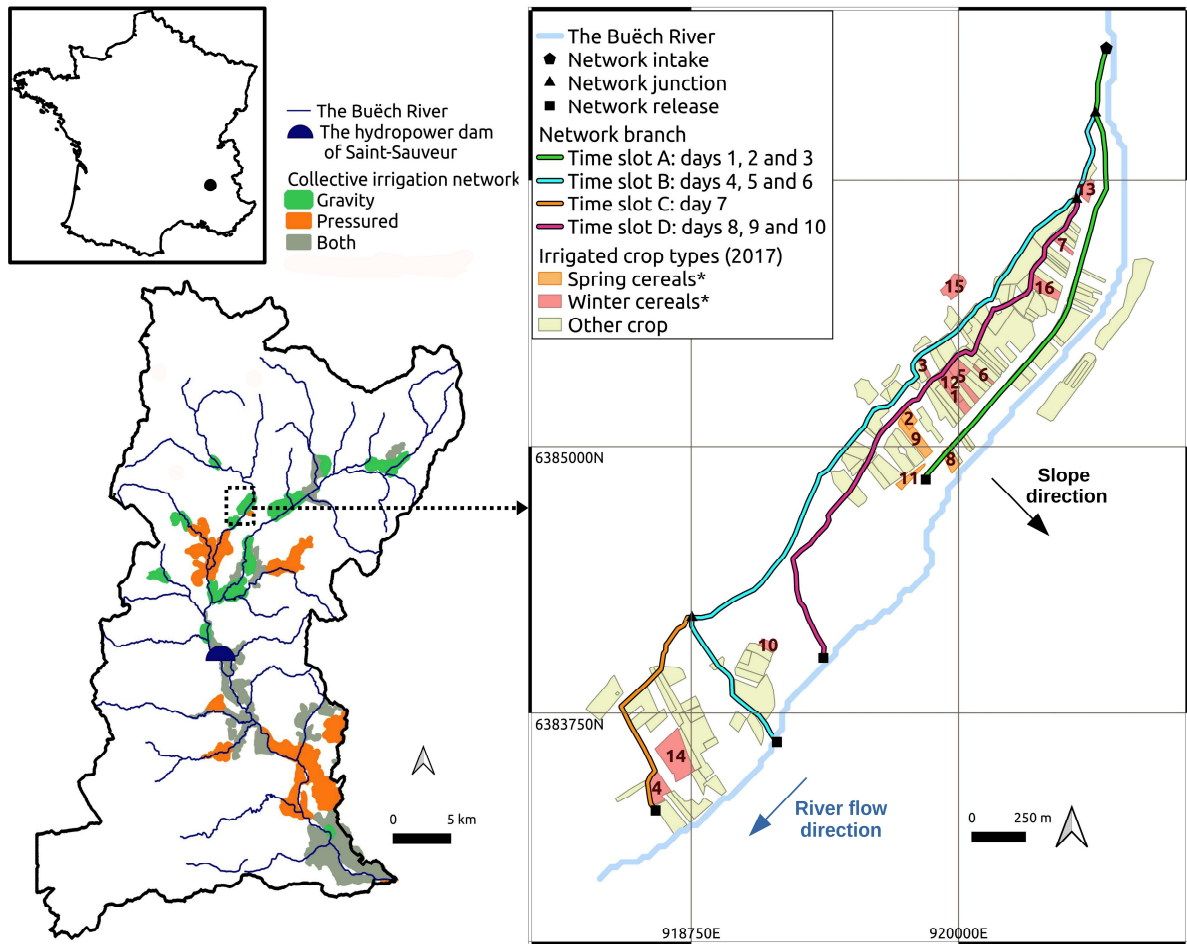


Fig. 2 (to be printed in color): Presentation of the Aspres-Sur-Buëch study area (right-side box) located in the Buëch River basin (left-side) in the South-East of France. Within the study area, the colors represent the types of crops irrigated by the gravity-fed network (source: BD Hydra V2 and RPG 2017). Bold numbers on the plots correspond to their identifiers. \* denotes crops simulated by the Optirrig-D model.

167 For practical reasons of crop model parameterization, we focus on 16 plots of cereal (Fig. 2,  
 168 right-side) made of 12 plots of winter cereal and 4 plots of springs cereal, that belong to 6 of the 10  
 169 irrigators sharing the gravity network. A description of the crop type, plot area and irrigator identifiers  
 170 of the 16 cereal plots is available in Supplementary materials. Irrigation on the other plots served by  
 171 the network is thus not driven by *TT* to be stopped at the end of the simulation period.

172 To verify that the co-simulation results are trustworthy, we conducted field surveys on the  
 173 study area as direct observation of irrigators' practices and semi-structured interviews about the  
 174 irrigation campaign that took place between May and September 2017. The interviews were  
 175 conducted with four irrigators, the technician in charge of the water network regulation, and the  
 176 President of the irrigator union as the information collected covered the entire irrigated command



177 area. The coordination of the gravity network through a daily slot calendar has been gradually  
 178 abandoned during the last 15 years as it was temporally very restrictive according to the  
 179 interviewees. We have captured the latest version in place, the one known to all the interviewees.  
 180 The branches of the canal were watered according to four time-slots (A, B, C, and D, Fig. 2). During  
 181 a time-slot, water flows only in the branches designated by the calendar (e.g. the green branch during  
 182 slot A, the blue branch during slot B, etc.). The different daily slots follow one after the other in ten  
 183 days. Currently, irrigators don't coordinate the water network anymore to trigger irrigation: the water  
 184 flows simultaneously and continuously in all the branches of the canal until the end of the irrigation  
 185 campaign. Other information collected is further detailed in Supplementary materials.

### 186 3.2 Optirrig-D: crop dynamics at the plot level

187 The Optirrig model is a two-layer structure in which the inner layer performs hydro-agronomic  
 188 calculations, having rewritten and modified the concepts originally present in the PILOTE model  
 189 (Mailhol et al., 1997, 2011; Khaledian et al., 2009; Feng et al., 2014) and now termed PILOTE-R as

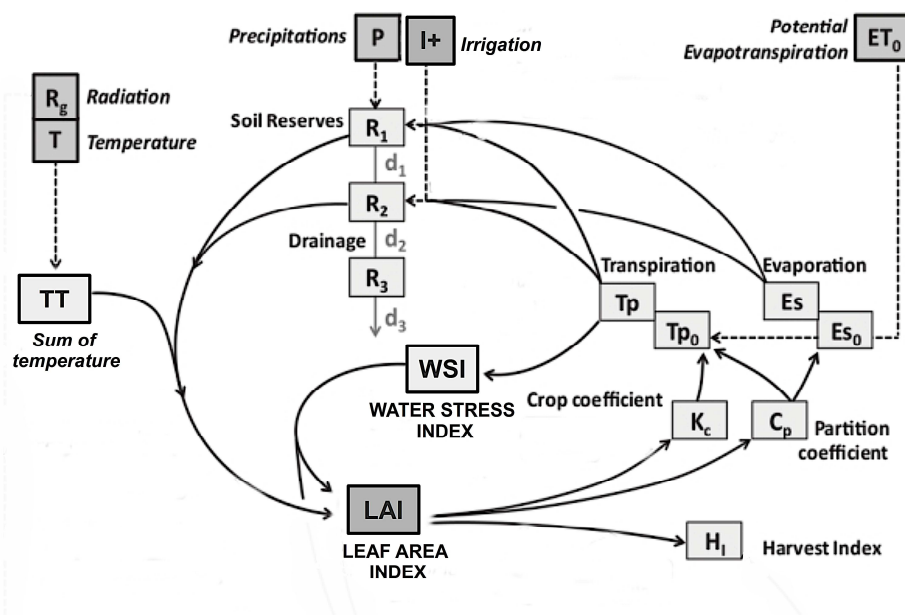


Fig. 3 (can be printed in black and white): Overview of the Optirrig model for the simulation of WSI and LAI variables (adapted from Cheviron et al., 2016). Climatic forcing are squares with thick contour lines, intermediate variables are pale grey sketches and key state variables are grey sketches with thick contours. Irrigation is noted  $I+$  to indicate that this model forcing depends on the irrigation decision-rules.

190 coded in the R language. The outer layer of Optirrig allows the use of multiple runs for various  
 191 numerical purposes, e.g. exploratory scenarios of irrigation and fertilization and/or climatic scenarios,  
 192 uncertainty and sensitivity analysis, model fitting or irrigation. Figure 3 gives an overview of the  
 193 structure and main variables of the model, among which are  $LAI$  and  $WSI$ .

194 The *Water Stress Index WSI* (the ratio between actual transpiration and maximal  
 195 transpiration), is calculated by the soil module as a moving average of 10 days. The *Leaf Area Index*  
 196 *LAI* simulation is performed using the following equation:

$$197 \quad LAI(j) = LAI_{max} \left[ \left( \frac{TT(j) - T_s}{t_f} \right)^\beta \exp \left( \frac{\beta}{\alpha} \left( 1 - \left( \frac{TT(j) - T_s}{t_f} \right)^\alpha \right) - \right. \right. \\
 198 \quad \left. \left. (1 - WSI^\lambda) \right) \right] \quad (\text{Eq. 1})$$

199 where  $TT(j) = \sum_{k=1}^{k=j} (T(k) - T_b)$  (Eq. 2)

200 and subscript  $j$  corresponds to a given *LAI* date,  $T(k)$  the average daily temperature of day  $k$ ,  
 201  $T_b$  the base temperature of the crop,  $LAI_{max}$  the maximum value of the *LAI* and  $T_s$  the temperature  
 202 of emergence,  $\alpha$  and  $\beta$  two shape parameters for *LAI* curves,  $WSI$  the water stress factor and  $\lambda$  a  
 203 parameter governing plant sensitivity to water stress. Complementary description of the soil and crop  
 204 modules of Optirrig are available in Supplementary materials.

205 Practically, we involved a recent version of the Optirrig model (Cheviron et al., 2016)  
 206 developed at INRAE G-Eau. This Optirrig-D version specifically developed for the co-simulation  
 207 approach (“D” denotes the specific daily horizon of simulation) allows the external forcing of irrigation  
 208 instructions for certain time steps, before the calculation of model state variables which are always  
 209 passed to the ABM at the end of the daily time step, whether irrigation takes place or not.

210 The Optirrig-D version developed in this study is thus a daily function derived from the Optirrig  
 211 model, which is usually run without interruption from the beginning to the end of the simulation period.  
 212 In this classical use, irrigation ( $I_+$ , in  $L \cdot m^{-2} \cdot d^{-1}$  in legal units, often given as mm) is either scheduled  
 213 according to decision rules, resulting in an irrigation calendar, or decided from field data and/or model  
 214 predictions, typically when the amount of water available in the root-zone reservoirs ( $R_1, R_2$ ) goes  
 215 under a certain threshold (see Supplementary materials). However, as the coupling with the ABM  
 216 requires forcing  $I_+$  according to agent actions, it is necessary to be able to modify it during the course  
 217 of the simulation, at each daily time step.

### 218 3.3 WatASit-Aspres: collective irrigation at the gravity network level

219 We use the ODD protocol (Grimm et al., 2006; 2010) to describe the model.

#### 220 3.4.1 Overview

221 The WatASit ABM is designed to simulate the irrigation operations of irrigators sharing a  
 222 common water network during a collective irrigation campaign. It explicitly represents the irrigation

223 options left by the network constraints of the irrigators. The constraints taken into account in WatASit-  
 224 Aspres are presented in Table 2. An irrigation possibility is generated on the plots where these  
 225 constraints make irrigation possible at a given hourly time step.

226 **Table 2:** *The gravity network constraints in the WatASit-Aspres model.*

Network constraint	Case study specification
Number of irrigators per farm	<i>One irrigator per farm</i>
Number of simultaneous irrigations per irrigator	<i>One irrigation at a time per irrigator</i>
Daily time window (maximum daily working time of each irrigator)	<i>12h</i>
Plot flood duration	<i>Fixed</i>
Target irrigation dose	<i>Fixed</i>
Required branch canal flow serving the plot floodgate	$\geq$ <i>plot flood rate (<math>Q_{flood}</math>)</i>
Functioning of the network while raining	<i>Irrigation is not triggered if there is precipitation</i>

227 **Entities**

228 The model is based on the distinction between the elements that are involved in irrigation  
 229 operations (called operational entities) and the areas over which operational entities can operate  
 230 (called spatial entities) which are the farm plot, the farm, and the irrigation scheme area. In the model,  
 231 the operational entities are the irrigator agents and the objects which are actionable by an irrigator  
 232 agent, such as the network branch, intake, junction and release points, the floodgate at each farm  
 233 plot, and the crops. The third kind of entity is an artifact that makes explicit some abstract things of  
 234 the real world such as options to irrigate, called affordances, resulting from the interactions between  
 235 an irrigator agent and a hydraulic object (typically a floodgate). Description of all entities is available  
 236 in Supplementary materials.

237 **Process overview and scheduling**

238 The model is based on a double-time step. Each day, there is first initialization of the current  
 239 precipitation conditions, and also of the number of days since the crops have not been irrigated.  
 240 Then, every hour, the flow is updated in the network according to network junction state  
 241 (i.e. "opened " or "closed ") and ended actions. Irrigation options are then generated on each farm.  
 242 Depending on the irrigator's decision-making rules (Fig. 4), an option can be chosen to make a flood  
 243 action or ask for more water in the canal. An activity diagram presenting process scheduling is  
 244 available in Supplementary materials, as well as detailed descriptions of the affordance generation  
 245 sub-model, action execution sub-model, and simplified hydraulic sub-model of the gravity network.

### 246 3.4.2 Design concepts

247 WatASit represents the phase of implementation of actions according to the theory of Situated  
248 Action (Dreyfus, 1972, Suchman, 1987). In the model, the behavior of the irrigator agents is  
249 determined by their options to irrigate, which are re-evaluated at each hourly time step. Each agent  
250 chooses none or one option among its set of options and performs it. When one agent has performed  
251 an option, sets of options of all agents need updating. Irrigator agents interact indirectly with each  
252 other by reducing the amount of water available in the network which affects the options of the other  
253 agents sharing the same or a downstream branch. Design concepts of the model are further detailed  
254 in Supplementary materials.

### 255 3.4.3 Details

256 The model, called WatASit-Aspres, has been already deployed to represent the Aspres-  
257 Sur-Buëch case study (Richard et al., 2020) for which the specific parameterization has been  
258 detailed. Spatial entities were initialized using a pre-processing that consists of rasterizing the farm  
259 plot shapefiles (Table 3) onto a 54x44 cell grid with a resolution of 75 m. The water network was also  
260 initialized using shapefiles (Table 3). At the initialization, farm plots served by the network were listed  
261 for each canal branch. Daily precipitation input comes from the French near-surface SAFRAN  
262 reanalysis (Vidal et al., 2010).

263 **Table 3:** Data type and sources for the initialization of the WatASit-Aspres model.

Data type	Data source
Daily precipitation	SAFRAN reanalysis (Vidal et al., 2010)
Farm plot shapefiles, areas and crop types	"Registre Parcellaire Graphique" (RPG) 2017 <sup>2</sup>
Water network shapefile	BD HYDRA (v2) 2015 <sup>3</sup>

264

### 265 3.5 Coupled model inputs and parameterization

266 As for WatASit, Optirrig-D inputs are the climatic forcing (precipitation, temperature, global  
267 radiation, and reference evapotranspiration) and were obtained from the French SAFRAN reanalysis  
268 (Vidal et al., 2010) from January 1, 2017, to December 31, 2017.

269 Parameters of both models are specified in Appendix A (Table A.1). Concerning Optirrig,  
270 typical parameters of winter soft wheat have been considered for all winter cereals. Parameters for  
271 spring cereals are based on typical spring oat parameters. For a given crop, literature (e.g. Cox and  
272 Joliff, 1986; Howell et al., 1996) can provide some parameters such as the  $LAI_{max}$ ,  $tf$ , and the  $TM$   
273 parameter. All these parameters are linked to the base temperature  $T_b$  parameter, which is also

2 A version 2.0 distributed since 2015 is directly accessible online at <http://professionnels.ign.fr/rpg>

3 Accessible online at <http://hydra.dynmap.com/index.php?grFrame=1>

274 given in relevant literature (see Mailhol et al., 1997). Sowing DOY are average dates reported by  
275 irrigators during the 2016-2017 crop campaign for the study area. Available water reserve (*AWR*)  
276 and maximum profile and rooting depth (*Pmax*) for the study area are from the PACA Regional Soil  
277 Reference System described in Braud et al. (2013). Moreover, *AWR* in the soil of the plots in the  
278 study area was calculated from the PACA Regional Soil Reference System using a method  
279 presented in Manus et al. (2009).

280 Concerning WatASit-Aspres, the key parameter is the target plot flood duration (*D*) as  
281 irrigation continues until reaching 4 hours for a plot area of 1 hectare. As the flow rate of the floodgate  
282 (*Qflood*, see Table A.1) is fixed, it is equivalent to inject a fixed irrigation dose of 43.2 mm per per  
283 day (*Idose*, see Table A.1). Other parameters are specific irrigation operations and gravity-fed  
284 network characteristics mentioned by the irrigators for the study area. In particular, the reference  
285 flow rate at the network intake (*Qref*, see Table B.1) was determined by the irrigators to avoid  
286 overflow and comply with the river abstraction rules during the 2017 low-flow period (also note that  
287 no irrigation restrictions came into effect during the 2017 cereal campaign).

288 Decision-making for irrigation consists in irrigating crops after several days without sufficient  
289 precipitation inputs to contain as much as possible a maximum of successive non-irrigated days (Fig.  
290 4). As water is not always sufficiently available to irrigate a plot, irrigator agents have three kinds of  
291 options: irrigate a plot with a *Flood* option, ask for increasing the water flow in the network with an  
292 *AskMoreWater* option, and do something else during this time step. Finally, a plot for which the  
293 irrigator has not had an option to irrigate for a certain period of time is abandoned for irrigation (see  
294 Fig. 4).

295

296

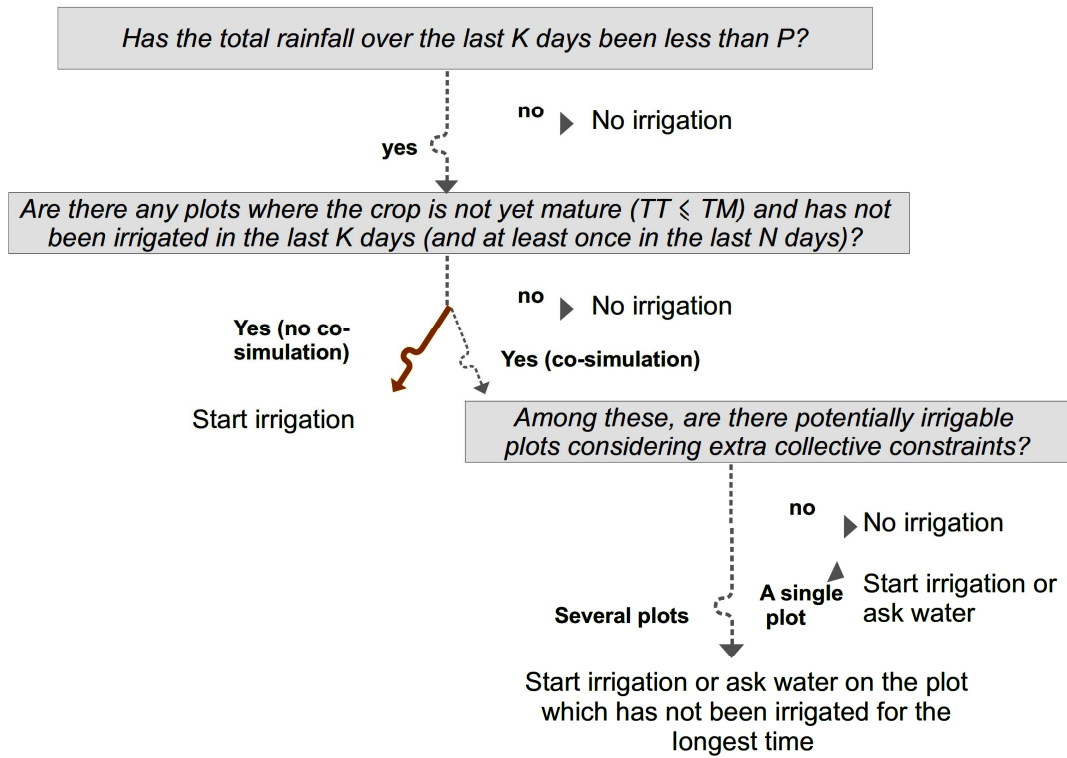


Fig. 4 (can be printed in black and white): Irrigation decision-rules considered for the case study. Typical values are  $K=12$  days,  $P=120$  mm,  $N=45$  days and  $TM=1200^{\circ}\text{C}$  for spring cereals and  $1700^{\circ}\text{C}$  for winter cereals.

297

### 298 3.6 Simulations

299 We simulated the 2017 retrospective irrigation campaign under four levels of collective  
 300 network constraints (Table 4). The co-simulation approach is used for simulating the space collective  
 301 constraint due to the sharing of water among irrigators through the gravity (Fig. 1 [b]). The time  
 302 collective constraint is represented by the time-slot-based coordination (described in Section 3.1 and  
 303 Fig. 2 right-side) for the study area, either in the ABM or directly implemented in the crop model.

304 **Table 4.** Levels of collective irrigation constraint to operate irrigation during the 2017 irrigation  
 305 campaign of the four simulation runs. The time collective constraint is the daily time-slot-based  
 306 coordination presented in Section 3.1 and Figure 2. The space collective constraint is the sharing of  
 307 water through the gravity network simulated by the WatASit-Aspres model with constraints detailed  
 308 in Table.

Simulation name	Abbreviation	Collective constraint type		Co-simulation
		Gravity network	Time-slot based coordination	

<i>No collective constraint</i>	<i>NoCollCons</i>	<i>No</i>	<i>No</i>	<i>No</i>
<i>Space collective constraint</i>	<i>SpaCollCons</i>	<i>Yes</i>	<i>No</i>	<i>Yes</i>
<i>Time collective constraint</i>	<i>TimCollCons</i>	<i>No</i>	<i>Yes</i>	<i>No</i>
<i>Space and time collective constraints</i>	<i>SpaTimCollCons</i>	<i>Yes</i>	<i>Yes</i>	<i>Yes</i>

309

310 We called “No collective constraint” (NoCollCons) the simulation in which irrigators optimally  
311 irrigate at the plot level without nor the spatial collective constraint due to the gravity network neither  
312 the time collective constraint due to the time-slot-based coordination. Irrigation is simulated at the  
313 plot level by the Optirrig-D model only (Fig. 1 [a]). This simulation thus shortcuts the WatASit-Aspres  
314 model during the whole simulation period, including the irrigation campaign. NoCollCons does not  
315 consider any possibility of conflict between irrigators for the sharing of water. Irrigation decisions are  
316 then equivalent to a regular plot-based calendar.

317 We called “Space collective constraint” (SpaCollCons) the simulation in which irrigation is  
318 simulated at the network level by the coupled models (Fig. 1 [b]) without the time collective constraint  
319 due to time-slot-based coordination. The sharing of water for the irrigation operations is spatially  
320 driven by the gravity network constraints (Table 2) that cannot allow distributing water everywhere at  
321 the same time. As irrigators do not coordinate the network, water flows simultaneously in all the  
322 branches of the gravity network during the irrigation campaign.

323 “Space and time collective constraints” (SpaTimeCollCons) is the simulation in which  
324 irrigation is simulated at the network level by the coupled models (Fig. 1 [b]), driven both by the  
325 gravity network constraints (Table 2) and by the time-slot-based coordination. It depicts flow  
326 coordination using a daily slot (i.e. A, B, C or D) for each network branch constraining temporally  
327 irrigation operations, as described in Section 3.1 and presented in Fig. 2 (right-side).

328 Finally, “Time collective constraint” (TimCollCons) is the simulation in which irrigators irrigate  
329 at the plot level following the time-slot based coordination but without the gravity network constraints.  
330 Irrigation is simulated at the plot level by the Optirrig-D model only (Fig. 1 [a]) with irrigation dates  
331 constrained by similar daily slots as in the SpaTimCollCons simulation, but directly generated in the  
332 Optirrig-D model.

333 The total simulation period runs from 15 October or Day of Year 1 (DOY 1), when the winter  
334 cereals are sown, to the end of the cereal season on July 31 (DOY 289). The co-simulation starts at  
335 the beginning of the irrigation campaign on May 1st (DOY 198) when irrigators of Aspres-Sur-Buëch  
336 water their network each year. 2017 is taken as a reference for the climatic forcing. Simulation output  
337 (i.e. dates of irrigation, *LAI*, *TT*, and *WSI* on each farm plot) are collected from the two models by  
338 recording attributes of WatASit-Aspres entities (i.e. irrigated state of farm plot entities) and Optirrig-

339 D variables (i.e. cereal *LAI*, *TT*, and *WSI*) in the R software during the irrigation campaign. In sections  
340 4.3 and 4.4, we also indicate an output from an extreme simulation run called “Nolrri” without any  
341 irrigation input during the irrigation campaign, as a benchmark. *WSI* equals 1 is corresponding to low  
342 plant water stress. Blue, yellow, orange and red colors denote low ( $WSI > 0.75$ ), medium ( $0.5 < WSI$   
343  $\leq 0.75$ , high ( $0.25 < WSI \leq 0.5$ ) and very high ( $WSI \leq 0.25$ ) water stress, respectively.

#### 344 **4. Simulation results**

##### 345 4.1 Irrigation dates for the four levels of gravity collective network constraints

346 This section presents the irrigation dates of the 16 cereal plots simulated for the four levels  
347 of collective irrigation network constraints (Table 4).

348 The two top lines NoCollCons and SpaCollCons of Figure 5 correspond to irrigation dates  
349 when the network is not coordinated. In the NoCollCons simulation, the plots are irrigated  
350 simultaneously on a regular 12-days basis until maturity temperature is reached (materialized by the  
351 green lines). This is not the case in the SpaCollCons simulation in which we observed significant  
352 delays between the series of irrigation, and no irrigation for the most downstream plots 10, 14 and  
353 4. For instance, 28 days separate the series of irrigation between DOY 207 and DOY 235. Taking  
354 into account the spatial network constraint thus leads to both the abandonment of the most  
355 downstream plots (i.e. plots 4, 10, and 14) and significant delays in series of irrigation. As a  
356 consequence of irrigation delays, maturity of the crops is reached later for some of the crops (e.g. 3  
357 and 4 days for plots 15 and 16, respectively) in the SpaCollCons simulation than in the NoCollCons.

358 The two bottom lines TimCollCons and SpaTimCollCons of Figure 5 correspond to irrigation  
359 dates when the network is coordinated. Irrigation operations simulated in the TimCollCons are  
360 distributed differently over time from one plot to another and form a pattern driven by the four A, B,  
361 C, and D slots that irregularly repeats until the maturity temperature is reached. In the  
362 SpaTimCollCons simulation, the pattern is not exactly repeated as irrigation operations are  
363 constrained both by daily slots and the gravity network constraints, notably the precipitation of the  
364 day (Table 2). However, reaching plant maturity is not necessarily penalized, and happens even  
365 earlier on some plots (2, 5, 6, 10, and 16).

366 Comparing the SpaCollCons and the SpaTimCollCons simulations, the plots are almost  
367 always irrigated at the same time when irrigation is not coordinated (SpaCollCons). But the absence  
368 of network coordination leads to significant delays from a series of irrigation to another, and a lack  
369 of irrigation in most downstream plots, which is prevented by the coordination of the network  
370 (SpaTimCollCons).



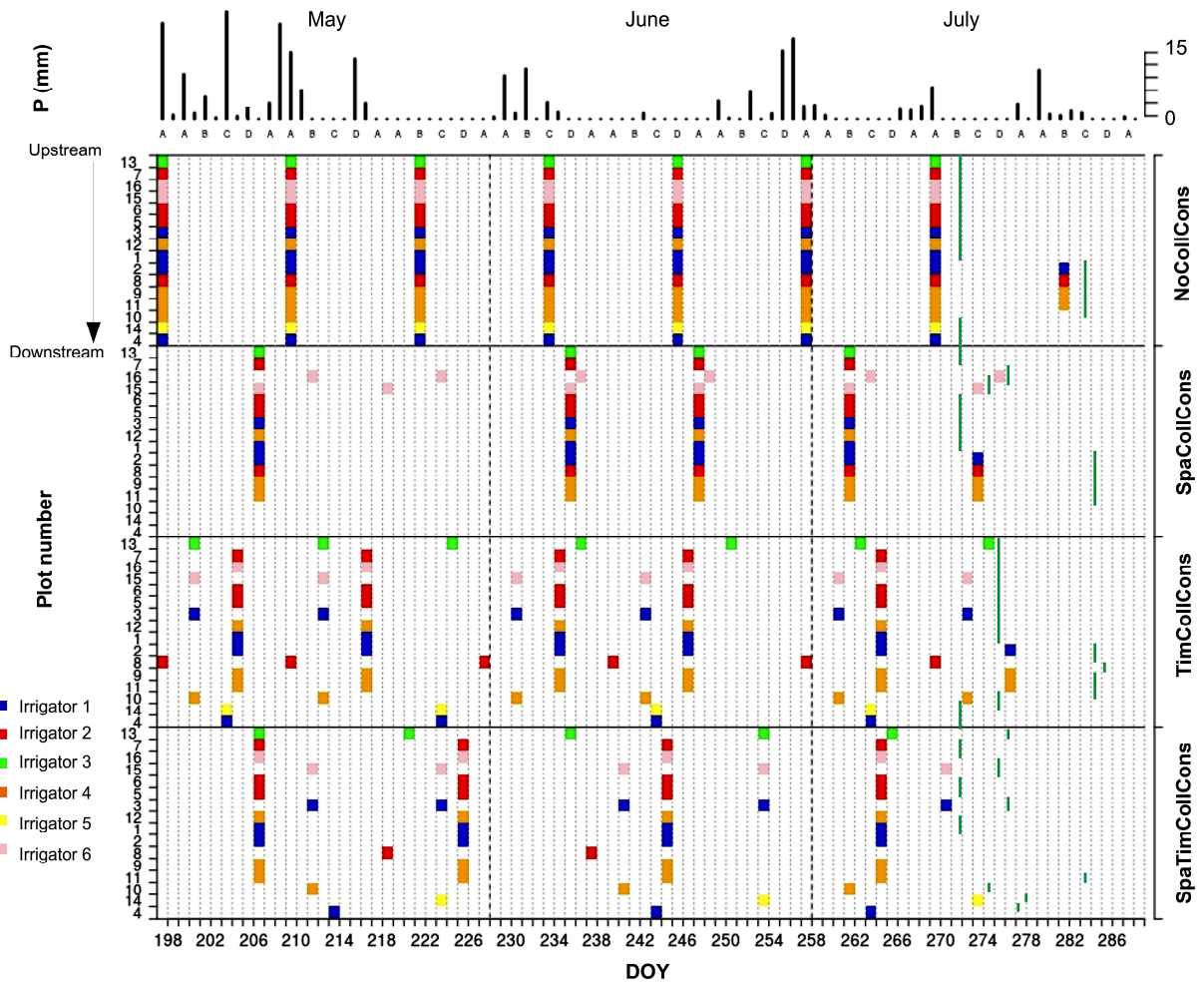


Fig. 5 (to be printed in color): Irrigation dates within the 16 cereal plots from May 1st (DOY = 198) to July 31 (DOY = 289). NoCollCons and TimCollCons are simulations at the plot level. SpaCollCons and SpaTimCollCons depict co-simulations at the network level. Colors are irrigator identifiers, black ticks are precipitation ( $P$ , in mm). “A”, “B”, “C”, and “D” labels indicate the coordination daily slots. Green ticks show when the maturity is reached by the plant.

#### 371 4.2 Elements of model validation

372 Results of the SpaCollCons retrospective simulation are consistent with the elements  
 373 identified during the field survey for the 2017 real irrigation campaign that took place as in the  
 374 SpaCollCons simulation in the absence of time-slot-based coordination of the network branches.  
 375 Namely, the plots located downstream of the gravity-fed network (cereal plots 10, 14, and 4) were  
 376 not irrigated at all during the 2017 irrigation campaign. The interviewees mentioned 4 irrigation dates  
 377 by plot for the middle plots (i.e. plots 2, 8, 9, and 11), and 5 for the upstream plots (i.e. the other  
 378 plots) during the cereal campaign, which is in line with the SpaCollCons simulation results. In  
 379 addition, harvest dates for the 2017 cereal campaign on the study area range from July 15<sup>th</sup> (DOY  
 380 273) to July 30<sup>th</sup> (DOY 288), which is very close to the simulation window for cereal maturity dates  
 381 ranging from July 14<sup>th</sup> (DOY 272) to July 26<sup>th</sup> (DOY 284).

#### 382 4.3 Potential impacts of the collective irrigation constraints on average LAI and WSI dynamics

383            This section focuses on the average LAI and WSI time-series integrated over the irrigation  
384 campaign (Fig. 6).

385            In the SpaCollCons simulation, the absence of network coordination (Fig. 6, *WSI*, green line)  
386 leads to earlier medium water stress on average (i.e. 10 days earlier) than when the network is also  
387 coordinated in the SpaTimCollCons simulation (orange line). The absence of coordination induces  
388 an impact on cereal growth: maximum of average *LAI* (Fig. 6, *LAI*, green line) is reached 12 days  
389 earlier and about 1 point lower than when the network is coordinated (green line). Irrigation  
390 operations are less frequent and less distributed over time in the absence of coordination (Fig. 6,  
391 irrigation number). The network specific constraints therefore significantly impact average crop water  
392 stress when the network is not coordinated, while network coordination tends to delay the impact  
393 over the irrigation campaign.

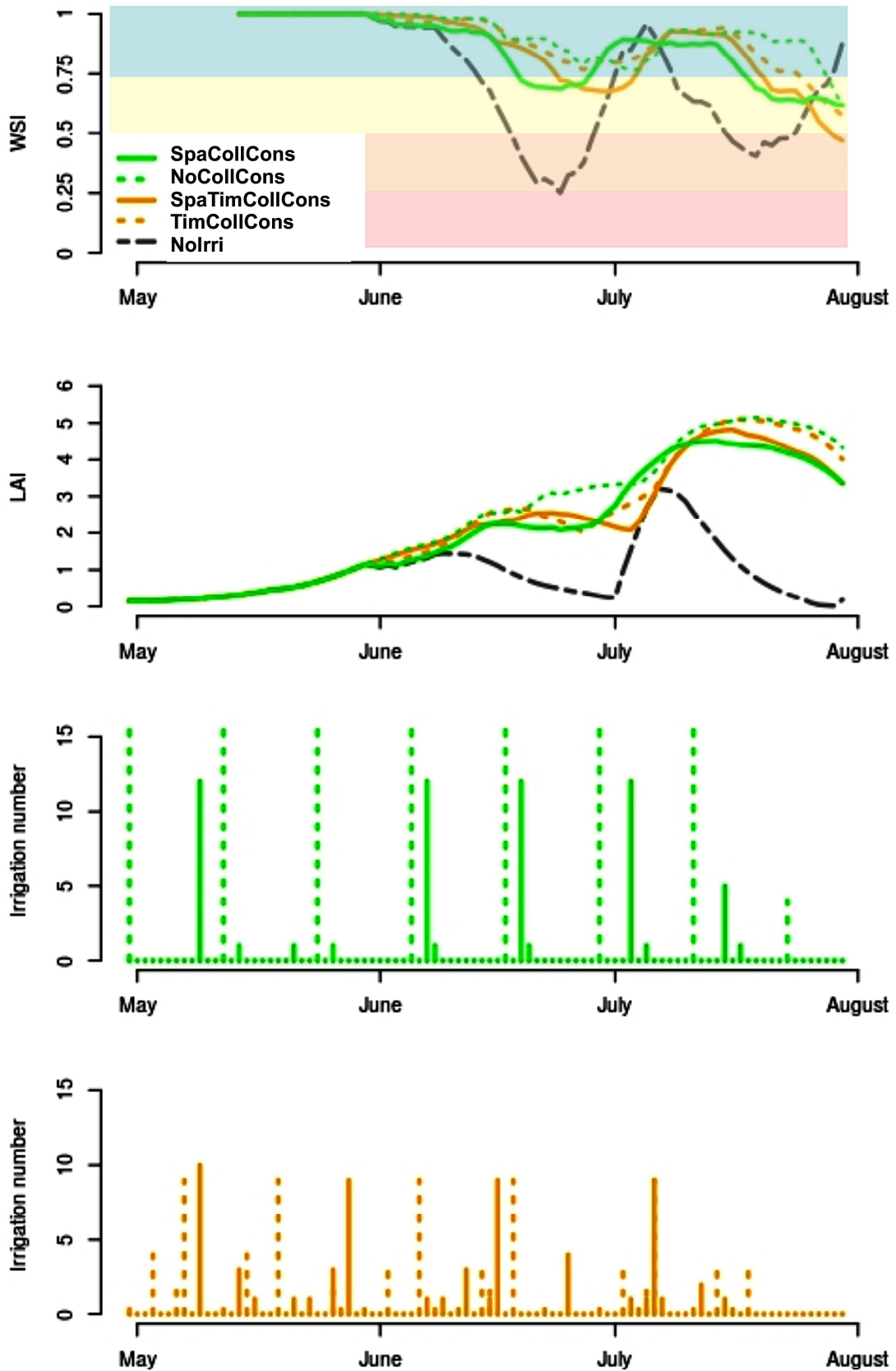
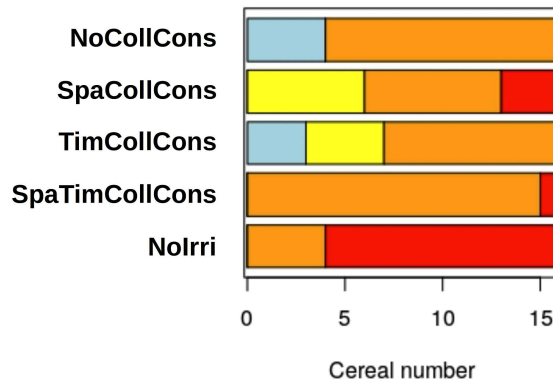


Fig. 6 (to be printed in color): LAI, WSI and irrigation number evolution for all cereals during the irrigation campaign from May 1st to July 31. Green and orange lines are the SpaCollCons and SpaTimCollCons simulations, respectively. Dotted green and orange lines are the NoCollCons and TimCollCons simulations, respectively. Background blue, yellow, orange and red colors indicates low, medium, high and very high plant water stress severity, respectively.

395 4.4 Spatial distribution of water stress severity at the irrigation network level

396 In this section, we measure the water stress severity of a cereal plot as the greatest stress  
397 level undergone by this cereal over a simulation. In Optirrig-D the time-evolution of *WSI* values is  
398 the consequence of both precipitation and irrigation events from the 10 past days, and *WSI* is the  
399 main control over *LAI* values. Since severe water stress has an exponential impact on biomass  
400 growth, it makes sense to locate it during the irrigation campaign

401 Figure 7 shows the cereal number for each water stress severity level and Figure 8 locates  
402 maximum stress severity within the 16 cereal plots. In the NoCollCons simulation, cereal maximum  
403 stress is low (blue plots) for all spring cereals and is high (orange plots) for all winter cereals. This  
404 difference is due to the Optirrig-D parameters that differentiate these two cereal types, especially the  
405 sowing period (see Appendix A). In the TimCollCons simulation, the coordination of the irrigation  
406 network induced fewer differences in cereal stress severity than in the NoCollCons simulation: three  
407 plots move from high to medium stress (Fig. 7, yellow plots). Daily slot coordination has thus a slight  
408 beneficial impact when irrigation is simulated without the specific gravity network constraints. In the  
409 absence of irrigation (NoIrr), winter cereals have dropped one class of maximum stress, from high  
410 to very high (Fig. 8, the red plots), and spring cereals have dropped two classes, with high stress  
411 (Fig. 8, the orange plots).



*Fig. 7 (to be printed in color): Cereal number for each water stress severity level. Blue, yellow, orange and red colors denote low ( $WSI > 0.75$ ), medium ( $0.5 < WSI \leq 0.75$ ), high ( $0.25 < WSI \leq 0.5$ ) and very high ( $WSI \leq 0.25$ ) stress, respectively.*

412 In the SpaCollCons simulation, a spatial dichotomy appears between the upstream part of  
413 the network, where stress severity is medium to high, and the downstream part, where all three  
414 cereal plots have very high maximum stress (Fig. 7 and Fig. 8). This dichotomy is not observed in  
415 the TimCollCons simulation and is less obvious in the SpaTimCollCons simulation when irrigation is  
416 simulated at the network level with daily slot coordination. In addition, maximum water stress globally  
417 occurs earlier when the network is not coordinated (Fig. 8, SpaCollCons).

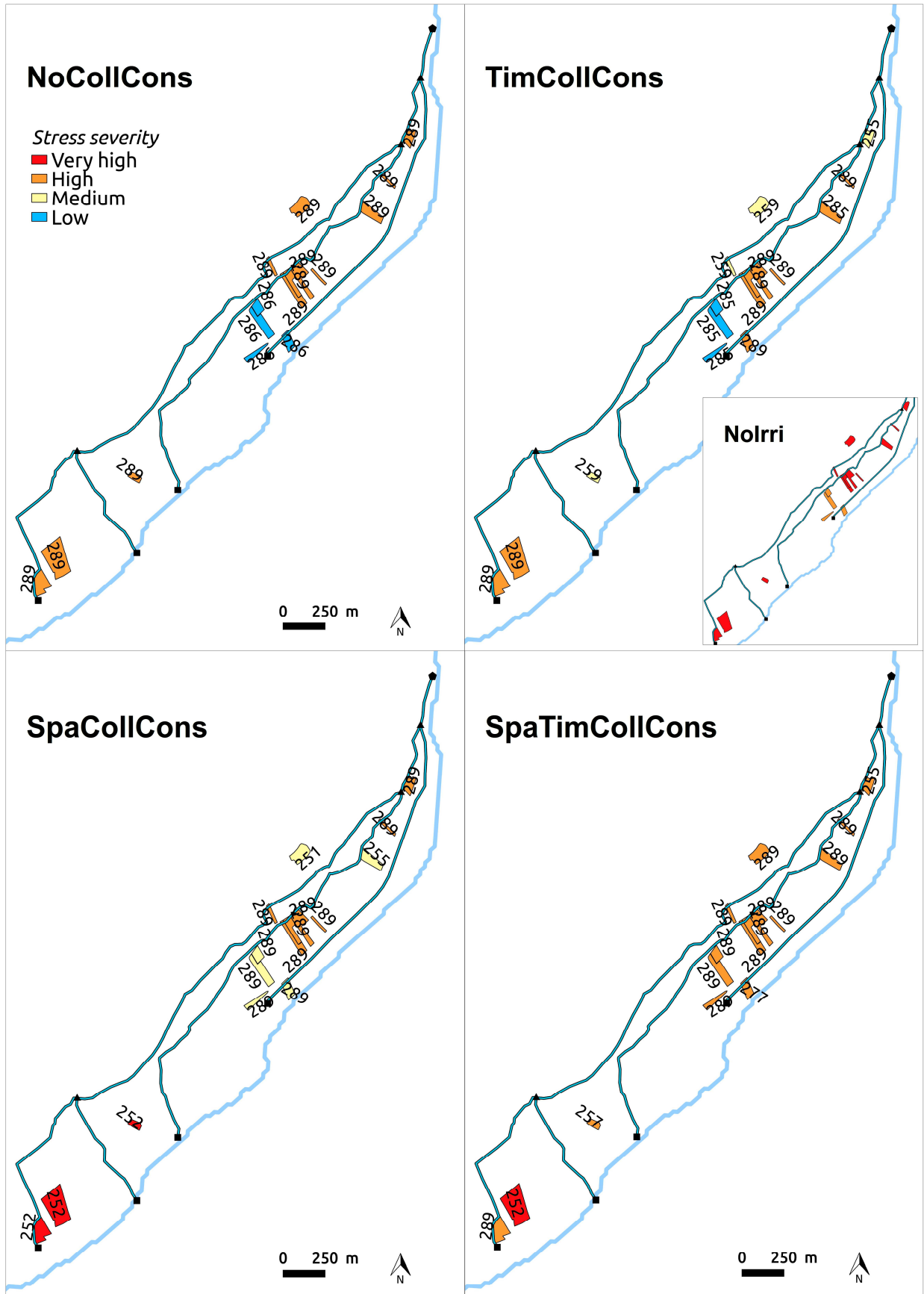


Fig. 8 (to be printed in color): Location of the maximum stress severity within the 16 cereal plots, according to the NoIrr, NoCollCons, TimCollCons, SpaCollCons and SpaTimCollCons simulations. Numbers are Days of Years of occurrence of the maximum water stress.

## 419 5. Discussion

420 In this section, we first discuss the proof of concept and the added value of the co-simulation  
421 approach for the study area. We also provide a sensitivity analysis to the key parameters. Then we  
422 consider the limitations of using coupled models and co-simulation, before presenting the key  
423 perspectives for future research.

### 424 5.1 Proof of concept and added-value of the co-simulation approach

425 Applied on a typical gravity network in South-Est of France, the co-simulation approach  
426 allowed to capture the potential impacts of the space and time constraints due to a gravity network  
427 on plant LAI and WSI dynamics in the study area. Compared to the first approach developed in  
428 Richard et al. (2020a) with the ABM alone, the co-simulation makes it possible to tackle the impact  
429 on some crop variables (i.e. *LAI*, *WSI*) widely used in agricultural system studies. The key point was  
430 the derivation of the crop model into a daily function, which made possible to run it as a slave model  
431 of the ABM during the course of the simulation, and thus to give daily irrigation orders at the plot  
432 level according to the collective sharing of water in the ABM.

433 The proof of concept also lies in comparing progressive levels of irrigation collective  
434 constraints on irrigation dates (Section 4.1), LAI and WSI dynamics (Section 4.3), and provides  
435 access to a tactical assessment of the spatial variability of plant water stress occurring at the network  
436 level during a collective irrigation campaign (Section 4.4). Simulation results highlight that network  
437 coordination tends to limit the impact of the gravity network constraint by delaying average plant  
438 water stress and increasing maximum average plant growth in comparison with simulation at the plot  
439 level. This is because the time-slot-based coordination reduces the effect of network flow along its  
440 upstream-downstream gradient, limiting missed irrigation for the most downstream plots, and thus  
441 reducing severe stresses on them.

442 Most approaches in the literature are merging crop models into a unique integrated simulation  
443 platform (e.g. Belcher et al., 2004; Raes et al., 2009; García-Vila and Fereres, 2012). As experienced  
444 by Marohn et al. (2013), coupling individual models in a co-simulation approach prevented  
445 simplifying many dynamics that are exogenous to the coupled model. For example, the precocity of  
446 plant water stress when the network is not coordinated (i.e. SpaCollCons simulation), as a result of  
447 irrigation delays caused by the network gravity constraint, could not have been represented by either  
448 model individually. The approach, therefore, enables the development of individual models  
449 simultaneously and independently, with people yet familiar with them.

### 450 5.2 Sensitivity analysis to key parameters

451 We performed a one-at-a-time exploration to assess the influence of key parameters (i.e. the  
452 maximum flow at the gravity network intake  $Q_{max}$ , the *flood duration* for irrigating 1 ha of plot, and  
453 the *time slot period* for the gravity network coordination) on the percentage of days with low, medium,  
454 high and very high plant water stress during the irrigation campaign. We changed parameter values

455 one at a time by letting the other parameters to their nominal values: *network intake flow* is  $0.09 \text{ m}^3$   
456  $\text{s}^{-1}$  (the river flow is considered as non-limiting), the *flood duration* is 4 hours per hectare, and the  
457 *daily slot period* is 10 days. We repeated each exploration run for the two SpaCollCons and  
458 SpaTimCollCons simulations that rely on the coupled models and co-simulation. Results are plotted  
459 in the graphic available in Supplementary materials.

460 The percentage of days with plant water stress during the irrigation campaign is not sensitive  
461 to the  $Q_{max}$  and *flood duration* parameter when the gravity network is coordinated  
462 (SpaTimCollCons). In the absence of network coordination (SpaCollCons), higher  $Q_{max}$  parameter  
463 value reduces plant water stress. The percentage of days with low plant water stress increases from  
464 83 to 87 when  $Q_{max}$  exceeds  $0.3 \text{ m}^3 \text{ s}^{-1}$ . The optimum of 87 days is reached when  $Q_{max}$  equals  
465  $0.35 \text{ m}^3 \text{ s}^{-1}$ . In addition, the percentage of days with medium, high and very high plant water  
466 stress is null when the *flood duration* parameter is 4 hours per hectare, that corresponds to the value  
467 mentioned by the irrigators for the study area. Concerning the effect of the modalities of network  
468 coordination through daily slots (i.e. the *time slot period* parameter), a period of 8 consecutive days  
469 (the two first days for *Slot A*, the next two days for *Slot B*, day 5 for *Slot C*, and the last 3 days for  
470 *Slot C*) seems to be slightly more advantageous than the other modalities for increasing the  
471 percentage of days with low plant water stress during the irrigation campaign.

### 472 5.3 Limitations of the co-simulation approach

473 As described by Letcher et al. (2013), the coupling of individual models is only possible under  
474 certain conditions. First, individual model components do not necessarily work on the same space  
475 and time scale, but disaggregation or aggregation must often be applied to link models. In our  
476 approach, the water network results from aggregation in the ABM of the elementary spatial entities  
477 (the plots). In addition, the ABM has also a double-time scale (hourly and daily). These double space  
478 and time scales make it possible to link daily irrigation at the plot level in the crop model, with the  
479 constrained operations at the network-scale.

480 Specific protocols and associated computer software and API exist to develop and merge  
481 models components in integrated development environment. A famous example is the Functional of  
482 such standard Mock-up Interface specification (FMI) and the FIDE environment (Cremona et al.,  
483 2016). Bulatewicz et al. (2010) who used similar standards for model linking called OpenMI raised  
484 several benefits of using such standard specifications methods. In our case, as a proof of concept  
485 of a specific coupling, we did not develop such generic components but our work is a first step for  
486 doing this since the model components that we developed provide almost the same API that the one  
487 that Bulatewicz et al. (2010) developed for the model components they developed (namely: get  
488 values, set values and advance simulation in time).

489 The level of detail should also be appropriate for a specific purpose otherwise the coupled  
490 model could be overly complex, with difficulty to identify feedback drivers and over-parameterization.  
491 In our approach, the chosen parameters have been kept as simple as possible. It distinguishes only

492 two classes of crops, summer and winter cereals, whereas it could be specific to each cereal variety  
493 (barley, wheat, etc.).

494 In addition, the inter-related operations between hay-mowing, garden watering, and irrigation  
495 has not been considered but could have a significant impact on gravity-fed irrigation (Merot et al.,  
496 2008). This could be achieved by adding an explicit representation of garden watering and mowing  
497 operations in the WatASit-Aspres model or using a crop model representing such operations.

## 498 5.4 Perspectives for future research

### 499 5.4.1 Complementary elements for model validation and genericity

500 For future research, validating further the coupled model to site-specific data can be  
501 addressed by comparing simulated *LAI* with *LAI* retrieved from optical or remote sensing techniques  
502 (e.g. Zheng and Moskal, 2009).

503 Deploying the co-simulation approach to another case study means that detailed information  
504 is required to set up the model parameters, potentially limiting the spatial scale. The conceptual  
505 structure of the ABM, designed to be as generic as possible, allows changing the major structural  
506 constraints. However, the use of different irrigation decision rules may require specific crop indicators  
507 to be coupled. For instance, in systems where irrigation is finely controlled, evapotranspiration or  
508 *AWR* are often used to pilot irrigation. Such variables could be easily retrieved from the crop model.

509 Coupling further specialized models to the system, as the SIC hydraulic model (Baume et al.,  
510 2005), could also be useful for the modeling in the study area where the representation of flow in the  
511 network is a key issue.

### 512 5.4.2 Using the co-simulation approach to study the feedback loop of plant dynamics on irrigation 513 practices

514 The proposed coupling is bi-directional, but the coupling from the crop model to the agent-  
515 based model is probably less impacting than the coupling from the agent-based model to the crop  
516 model. Indeed, we dictated crop dynamics by forcing irrigation from the agents but only precipitation  
517 *P* and sum of temperature *TT* come from the crop model to drive the agent's behaviors (see Fig. 1  
518 [b]). Reinforcing the coupling from the crop model to the agent-based model could allow studying  
519 the feedback loop of plant dynamics on irrigation practice adaptation. It could be achieved by  
520 integrating, for example, the *WSI* variable in the irrigation decision-rules, as a proxy for crop water  
521 stress.

522 However, rather than looking at *WSI* which is an elaborated variable, and which corresponds  
523 to a conceptual representation, we could also reason in the percentage of the available water reserve  
524 *AWR* which is a phenomenological variable and concretely observable (sensors in the ground). This  
525 would avoid the *WSI* threshold phenomenon: when *WSI* decreases from 1 to *X*, no effect, then the  
526 effect is exponential when *WSI* decreases from *X* to 0 (especially if we reason on *WSI* averaged



527 over time, and even more so over long periods). This is why we used *WSI* classes in sections 4.3  
528 and 4.4 rather than comparing values directly.

#### 529 5.4.3 Requirements to be addressed for achieving an operational approach

530 The co-simulation approach entails the optimization of gravity irrigation networks in terms of  
531 retrospective analysis. A follow-up of this work could be to assess variants of the daily slots  
532 coordination to determine optimal coordination modalities for maximizing plant growth or minimizing  
533 crop water stress during an irrigation campaign.

534 The impact of such irrigation network optimization could be evaluated in terms of criteria such  
535 as water productivity, crop yield, or water-saving per season. As agricultural yield can be simulated  
536 by the crop model with extra parameters (e.g. plot density) it would be possible to establish the link  
537 between the maximum plant water stress that has occurred during an irrigation campaign and the  
538 final yield obtained. This could be of interest to make a cost-benefit analysis of different irrigation  
539 solutions. Overall, to be performed in an operational mode for optimizing an irrigation network in real-  
540 time conditions, the approach should integrate climatic forcing forecasts, and be further validated to  
541 site-specific data.

## 542 **6. Conclusions**

543 In this study, we proposed a co-simulation approach to tackle the potential impacts on crop  
544 growth and water stress of four progressive levels of spatial and temporal constraints due to a gravity  
545 irrigation. The approach relies on the coupling of a crop model at the plot level with an ABM at the  
546 network level. As a proof of concept, we applied it on a typical gravity network in South-East of  
547 France. Four progressive levels of collective irrigation constraints were simulated (i.e. no collective  
548 constraints, space collective constraints, time collective constraints, and space and time collective  
549 constraints). Retrospective simulation of the 2017 irrigation campaign is consistent with field surveys,  
550 and simulation results suggest that plant water stress could be underestimated when simulated at  
551 the plot level rather than at the network level. The co-simulation approach provides access to a  
552 tactical assessment of the spatial variability of plant water stress occurring during a collective  
553 irrigation campaign. Spatially, the most severe water stress was observed for the plants located  
554 furthest downstream of the network. Temporally, the absence of network coordination can lead to  
555 earlier plant water stress and lower plant growth during the collective irrigation campaign, while time-  
556 slot-based coordination tends to delay the impact. For future research, reinforcing the coupling from  
557 the crop model to the agent-based model could allow to study the feedback loop of plant dynamics  
558 on irrigation practice adaptations. It is also a first step towards an optimization approach for irrigation  
559 networks.

## 560 **Acknowledgment**

561 The authors would like to thank the Zone Atelier Bassin du Rhône (ZABR) and Agence de  
562 l'Eau Rhône-Méditerranée-Corse for funding the RADHY Buëch project to which this work

563 contributes. We also thank Météo-France for providing the SAFRAN reanalysis. The authors are  
564 grateful to the irrigators of Aspres-Sur-Buëch, all State Services, and associated structures of the  
565 Hautes-Alpes County, Claire Distinguin, for providing help during field surveys, and Jean-Claude  
566 Mailhol, for his explanations of the PILOTE model. Finally, the authors thank the anonymous  
567 reviewers.

## 568 **References**

569 Allen, R.G., Smith, M., Perrier, A. and Pereira, L.S., 1994. An update for the calculation of the  
570 reference evapotranspiration. *ICID Bull.* 43 (2): 1–31.

571 Aurbacher, J., Parker, P.S., Calberto Sánchez, G.A., Steinbach, J., Reinmuth, E., Ingwersen, J. and  
572 Dabbert, S., 2013. Influence of climate change on short term management of field crops – A  
573 modelling approach. *Agric. Syst.* 119: 44-57. <https://doi.org/10.1016/j.agry.2013.04.005>.

574 Baume, J.P., Malaterre, P.O., Belaud, G. and Le Guennec, B., 2005. SIC: un modèle  
575 hydrodynamique 1D pour la modélisation et la régulation des rivières et des canaux d'irrigation.  
576 *Métodos Numéricos em Recursos Hídricos.* 7: 1-81. hal-02587182.

577 Belcher, K.W., Boehm, M.M. and Fulton, M.E., 2004. Agroecosystem sustainability: a system  
578 simulation model approach. *Agric. Syst.* 79: 225-241.

579 Berger, T., Schreinemachers, P. and Woelcke, J., 2006. Multi-agent simulation for development of  
580 less-favored areas. *Agric. Syst.* 88: 28-43.

581 Berntsen, J., Petersen, B.M., Jacobsen, B.H., Olsen, J.E. and Hutchings, N.J., 2003. Evaluating  
582 nitrogen taxation scenarios using the dynamic whole farm simulation model FASSET. *Agric. Syst.* 76  
583 (3): 817-839.

584 Bithell, M. and Brasington, J., 2009. Coupling agent-based models of subsistence farming with  
585 individual-based forest models and dynamic models of water distribution. *Environ. Modell. Software.*  
586 24: 173-190.

587 Bommel, P., Bécu, N., Le Page, C. and Bousquet, F., 2015. Cormas, an Agent-Based simulation  
588 platform for coupling human decisions with computerized dynamics. In, T. Kaneda, H. Kanegae, Y.  
589 Toyoda and P. Rizzi (Éd.), *Simulation and Gaming in the Network Society.* Volume 9 of the series  
590 *Translational Systems Sciences*, pp 387-410. Springer Singapore. DOI: 10.1007/978-981-10-0575-  
591 6\_27.

592 Bousquet, F. and Le Page, C., 2004. Multi-agents simulations and ecosystem management : a  
593 review. *Ecological Modelling*, 176 :313-332.

594 Braud, I., Tilmant, F., Samie, R. and Le Goff, I., 2013. Assessment of the SiSPAT SVAT model for  
595 irrigation estimation in south-east France. *Procedia Environmental Sciences.* 19: 747-756. Doi:  
596 10.1016/j.proenv.2013.06.083.

597 Brisson, N., Gary, C., Justes, E., Roche, R., Mary, B., Ripoche, D., Zimmer, D., Sierra, J., Bertuzzi,  
598 P., Burger, P., Bussi re, F., Cabidoche, Y.M., Cellier, P., Debaeke, P., Guadill re, J.P., H nnault, C.,  
599 Maraux, F., Seguin, B. and Sinoquet, H., 2003. An overview of the crop model STICS. *Eur. J. Agron.*  
600 18: 309-332.

601 Bulatewicz, T., Yang, X., Peterson, J.M., Staggenborg, S., Welch, S.M. and Steward, D.R., 2010.  
602 Accessible integration of agriculture, groundwater, and economic models using the Open Modeling  
603 Interface (OpenMI): methodology and initial results. *Hydrol. Earth Syst. Sci.* 14: 521-534.

604 de Wit, A., 2015. PCSE documentation. Release 5, 80. [https://](https://media.readthedocs.org/pdf/pcse/latest/pcse.pdf)  
605 [media.readthedocs.org/pdf/pcse/latest/pcse.pdf](https://media.readthedocs.org/pdf/pcse/latest/pcse.pdf) (accessed 15 June 2020).

606 Cheviron, B., Vervoot, R.W., Alsbasha, R., Dairon, R., Le Priol, C. and Mailhol, J.C., 2016. A  
607 framework to use crop models for multi-objective constrained optimization of irrigation strategies.  
608 *Environ. Modell. Softw.* 86: 145-157.

609 Constantin, J., Willaume, M., Murgue, C., Lacroix, B. and Therond, O., 2015. The soil-crop models  
610 STICS and AqYield predict yield and soil water content for irrigated crops equally well with limited  
611 data. *Agric. For. Meteorology.* 206: 55-68.

612 Cox, W.J. and Joliff, G.D., 1986. Growth and yield of sunflower and soybean under soil water deficit.  
613 *Agron. J.* 78: 226–230.

614 Cros, M.J., Duru, M., Garcia, F. and Martin-Clouaire, R., 2004. Simulating management strategies:  
615 the rotational grazing example. *Agric. Syst.* 80: 23-42.

616 Cremona, F., Lohstroh, M., Tripakis, S., Brooks, C. and Lee, E.A., 2016. FIDE: an FMI integrated  
617 development environment. In *Proceedings of the 31st Annual ACM Symposium on Applied*  
618 *Computing (SAC '16)*. Association for Computing Machinery, New York, NY, USA, 1759–1766.

619 Dragan, M., Feoli, E., Ferneti, M. and Zerihun, W., 2003. Application of a spatial decision support  
620 system (SDSS) to reduce soil erosion in northern Ethiopia. *Environ. Modell. Software.* 18: 861-868.

621 Dreyfus, H.L., 1972. What computers can't do. A critique of artificial reason. New York: Harper and  
622 Row (Revised edition (1979). Augmented edition (1992), What Computers Still Can't Do. Cambridge,  
623 MA: MIT Press).

624 Feng, L., Mailhol, J.-C., Rey, H., Griffon, S., Auclair, D. and De Reffye, P., 2014. Comparing an  
625 empirical crop model with a functional structural plant model to account for individual variability. *Eur.*  
626 *J. Agron.* 53: 16-27.

627 Filatova, T., Verbug, P., Parker, D. and Stannard, C., 2013. Spatial agent-based models for socio-  
628 ecological systems: challenges and prospects. *Environmental Modelling and Software*, 45:1-7.

629 Garc a-Vila, M. and Fereres, E., 2012. Combining the simulation crop model AquaCrop with an  
630 economic model for the optimization of irrigation management at farm level. *Eur. J. Agron.* 36 (1):  
631 21-31.

632 Garcia, F., Guerrin, F., Martin-Clouaire, R. and Rellier, J.P., 2005. The human side of agricultural  
633 production management - the missing focus in simulation approaches. In: Zerger, A., Argent, R.M.,  
634 (Eds.). Proceedings of the MODSIM 2005 International Congress on Modelling and Simulation.  
635 Melbourne, Australia, 12-15 December 2005, pp. 203-209.

636 Gaudou, B., Sibertin-blanc, C., Therond, O., Amblard, F., Arcangeli, J., Balestrat, M., Sauvage, S.  
637 and Taillandier, P., 2013. The MAELIA multi-agent platform for integrated assessment of low-water  
638 management issues. In: MABS 2013 -14th International Workshop on Multi-agent-based Simulation.  
639 Saint Paul, Minnesota, pp. 1-12.

640 Grimm, V., Berger, U., Bastiansen, F., Eliassen, S., Ginot, V., Giske, J., Goss-Custard, J., Grand, T.,  
641 Heinz, S.K., Huse, G., Huth, A., Jepsen, J.U., Jørgensen, C., Mooij, W.M., Müller, B., Pe'er, G., Piou,  
642 C., Railsback, S.F., Robbins, A.M., Robbins, M.M., Rossmanith, E., Rüger, N., Strand, E., Souissi,  
643 S., Stillman, R.A., Vabø, R., Visser, U. and DeAngelis, D.L., 2006. A standard protocol for describing  
644 individual-based and agent-based models. *Ecol. Modell.* 198: 115-126.

645 Grimm, V., Berger, U., DeAngelis, D. L., Polhill, J. G., Giske, J., & Railsback, S. F. (2010). The ODD  
646 protocol: a review and first update. *Ecological Modelling*, 221, 2760–2768.  
647 <https://doi.org/10.1016/j.ecolmodel.2010.08.019>.

648 Guerrin, F., Afoutni, Z. and Courdier, R., 2016. Agent-based modeling: What matters is action. In The  
649 8<sup>th</sup> International Congress on Environmental Modelling and Software Society, iEMSs, pp. 412-419.  
650 Toulouse, France: Ed. Cepadues.

651 HarvestChoice, 2010. Generic Soil Profiles for Crop Modeling Applications (HC27). International  
652 Food Policy Research Institute, Washington DC, and University of Minnesota, St. Paul, MN. Available  
653 online at: <http://harvestchoice.org/node/662> (accessed 15 June 2020).

654 Howell, T.A., Evert, S.R., Tolk, J.A., Schneider, A.D. and Steiner, J.L., 1996. Evapotranspiration of  
655 corn-southern high plains. In: Proceedings of ASAE, San Antonio, Texas, 3–7 November, pp. 1–2.

656 Janssen, S. and van Ittersum, M.K., 2007. Assessing Farm Innovations and Responses to Policies:  
657 A Review of Bio-Economic farm Models. *Agric. Syst.* 94: 622-636.  
658 <https://doi.org/10.1016/j.agsy.2007.03.001>.

659 Johnston, W.H., Cornish, P.S. and Shoemark, V.F., 2005. *Eragrostis curvula* (Schrad.) Nees.  
660 Complex pastures in southern New South Wales, Australia: a comparison with *Medicago sativa* L.  
661 and *Phalaris aquatica* L. pastures under rotational grazing. *Aust. J. Exp. Agric.* 45(4): 401-420.

662 Jones, H.G., 1992. *Plants and Microclimate*, 2<sup>nd</sup> edn (Cambridge: Cambridge University Press),  
663 pp.428.

664 Jones, J.W., Hoogenboom, G., Porter, C.H., Boote, K.J., Batchelor, W.D., Hunt, L.A., Wilkens, P.W.,  
665 Singh, U., Gijsman, A.J. and Ritchie, J.T., 2003. DSSAT cropping system model. *Eur. J. Agron.* 18:  
666 235-265.

667 Keating, B.A., Carberry, P.S., Hammer, G.L., Probert, M.E., Robertson, M.J., Holzworth, D., Huth,  
668 N.I., Hargreaves, J.N.G., Meinke, H., Hochman, Z., McLean, G., Verburg, K., Snow, V., Dimes, J.P.,  
669 Silburn, M., Wang, E., Brown, S., Bristow, K.L., Asseng, S., Chapman, S., McCown, R.L., Freebairn,  
670 D.M. and Smith, C.J., 2003. An overview of APSIM, a model designed for farming systems  
671 simulation. *Eur. J. Agron.* 18: 267-288.

672 Letcher, R.A., Jakeman, A.J., Barreteau, O., Borsuk, M.E., ElSawah, S., Hamilton, S.H., Henriksen,  
673 H.J., Kuikka, S., Maier, H.R., Rizzoli, A.E, van Delden, H. and Voinov, A.A., 2013. Selecting among  
674 five common modelling approaches for integrated environmental assessment and management.  
675 *Environ. Modell. Software.* 47: 159-181. <https://doi.org/10.1016/j.envsoft.2013.05.005>.

676 Khaledian, M.R., Mailhol, J.C., Ruelle, P. and Rosique, P., 2009. Adapting PILOTE model for water  
677 and yield management under direct seeding system. The case of corn and durum wheat in  
678 mediterranean climate. *Agric. Water Manag.* 96: 757-770.

679 Mailhol, J.C., Ruelle, P., Revol, P., Delage, L. and Lescot, J.M., 1996. Operative modeling for  
680 evapotranspiration assessment: calibration methodology. In: ASAE Proceeding San Antonio (Texas),  
681 November.

682 Mailhol, J.C., Olufayo, O. and Ruelle, P., 1997. AET and yields assessments based on the LAI  
683 simulation. Application to sorghum and sunflower crops. *Agric. Water Manag.* 35: 167-182.

684 Mailhol, J.C., Ruelle, P., Walser, S., Schütze, N. and Dejean, C., 2011. Analysis of AET and yield  
685 prediction under surface and buried drip irrigation systems using the crop model PILOTE and Hydrus  
686 2D. *Agric. Water Manag.* 98: 1033-1044.

687 Matthews, R., 2006. The People and Landscape Model (PALM): towards full integration of human  
688 decision-making and biophysical simulation models. *Ecol. Modell.* 194: 329-343.

689 Matthews, R., Gilbert, N., Roach, A., Polhill, J. and Gotts, N., 2007. Agent-based land-use models:  
690 a review of applications. *Landscape Ecology*, 22:1447-1459.

691 Manus, C., Anquetin, S., Braud, I., Vandervaere, J.P., Viallet, P., Creutin, J.D. and Gaume, E., 2009.  
692 A modelling approach to assess the hydrological response of small Mediterranean catchments to  
693 the variability of soil characteristics in a context of extreme events. *Hydrol. Earth Syst. Sci.* 13: 79-  
694 87.

695 Marohn, C., Schreinemachers, P., Quang, D.V., Berger, T., Siripalangkanont, P., Nguyen, T.T. and  
696 Cadisch, G., 2013. A software coupling approach to assess low-cost soil conservation strategies for  
697 highland agriculture in Vietnam. *Environ. Modell. Software.* 45: 116-128.  
698 <https://doi.org/10.1016/j.envsoft.2012.03.020>.

699 Martin-Clouaire, R. and Rellier, J., 2009. Modeling and simulating work practices in agriculture.  
700 *IJMSO.* 4: 42-53.

701 McCown, R.L., Hammer, G.L., Hargreaves, J.N.G., Holzworth, D. and Huth, N.I., 1995. APSIM - an  
702 agricultural production system simulation model for operational research. *Math. Comput. Simul.* 39:  
703 225-231.

704 Merot, A., Bergez, J-E., Capillon, A. and Wery, J., 2008. Analysing farming practices to develop a  
705 numerical, operational model of farmers' decision-making processes: An irrigated hay cropping  
706 system in France. *Agricultural Systems*. 98(2):108-118. <https://doi.org/10.1016/j.agsy.2008.05.001>.

707 Monteith, J. L., 1977. Climate and the efficiency of crop production in Britain. *Philosophical*  
708 *Transactions of the Royal Society of London, Series B* 281: 277–294.

709 Murgue, C., Lardy, R., Vavasseur, V., Leenhardt, D. and Therond, O., 2014. Fine spatio-temporal  
710 simulation of cropping and farming systems effects on irrigation withdrawal dynamics within a river  
711 basin. In: Ames, Daniel P., Quinn, Nigel W.T., Rizzoli, Andrea E. (Eds.), 7th Int. Congress on Env.  
712 Modelling and Software (IEMSS), San Diego, CA, USA, p. 8.

713 Nolot, J.M. and Debaeke, P., 2003. Principes et outils de conception, conduite evaluation de  
714 systèmes de culture. *Cah. L'Agric.* 12: 387-400.

715 Parker, D.C., Manson, S.M., Janssen, M.A., Hoffmann, M.J. and Deadman, P., 2003. Multi-agent  
716 systems for the simulation of land-use and land-cover change: a review. *Ann. Assoc. Am. Geogr.* 93:  
717 314-337.

718 Raes, D., Steduto, P., Hsiao, T.C. and Fereres, E., 2009. AquaCrop the FAO crop model to simulate  
719 yield response to water. II. Main algorithms and software description. *Agron. J.* 101: 438-447.

720 R Core Team, 2018. R: A language and environment for statistical computing. R Foundation for  
721 Statistical Computing, Vienna, Austria. <http://www.R-project.org> (accessed 15 June 2020).

722 Reidsma, P., Ewert, F., Boogaard, H. and Diepen, K.V., 2009. Regional crop modelling in Europe:  
723 the impact of climatic conditions and farm characteristics on maize yields. *Agric. Syst.* 100 (1-3): 51-  
724 60.

725 Richard, B., Bonte, B., Barreteau, O. and Braud, I., 2020a. The abandonment of water daily slot and  
726 its operational consequences on collective irrigated systems. A situational multi-agent approach  
727 applied to a gravity-fed canal of Middle-Durance (France). *La Houille Blanche.* 4:43-55.  
728 <https://doi.org/10.1051/lhb/2020033>.

729 Richard, B., Bonte, B., Barreteau, O., Braud, I., 2020b, July 28. "WatASit" (Version 1.2.0). CoMSES  
730 Computational Model Library. Retrieved from: [https://www.comses.net/codebases/0d8dcaf1-8772-  
731 4e57-9f03-1f6c062bbe60/releases/1.2.0/](https://www.comses.net/codebases/0d8dcaf1-8772-4e57-9f03-1f6c062bbe60/releases/1.2.0/) (accessed 28 July 2020).

732 Schreinemachers, P., Berger, T. and Aune, J.B., 2007. Simulating soil fertility and poverty dynamics  
733 in Uganda: a bio-economic multi-agent systems approach. *Ecol. Econ.* 64: 387-401.

- 734 Schreinemachers, P., Potchanasin, C., Berger, T. and Roygrong, S., 2010. Agent-based modeling  
735 for ex-ante assessment of tree crop technologies: litchis in northern Thailand. *Agric. Econ.* 41: 519-  
736 536.
- 737 Sebillote, M. and Soler, L.G., 1990. Les processus de décision des agriculteurs. *Acquis et questions*  
738 *vives*. In : Brossier, J., Vissac, B., Le Moigne, J. L. (éds.) *Les systèmes de culture*. Paris, INRA, coll.  
739 *Un point sur...*, pp. 165-196.
- 740 Snow, V. and Lovatt, S., 2008. A general planner for agroecosystem models. *Computers and*  
741 *electronics in agriculture*. 60: 201-211. DOI: [10.1016/j.compag.2007.08.001](https://doi.org/10.1016/j.compag.2007.08.001).
- 742 Steduto, P., Hsiao, T.C., Raes, D. and Fereres, E., 2009. AquaCrop the FAO crop model to simulate  
743 yield response to water. I. Concepts and underlying principles. *Agron. J.* 101: 426:437.
- 744 Suchman, L., 1987. *Plans and situated actions: the problem of human/ machine communication*.  
745 Cambridge: Cambridge University Press. Turvey MT. 1992. *Affordances and prospective control: an*  
746 *outline of the ontology*. *Ecol Psychol.* 4: 173–187.
- 747 Supit, I., van Diepen, C.A., de Wit, A.J.W., Wolf, J., Kabata, P., Baruth, B. and Ludwig, F. 2012.  
748 *Assessing climate change effects on European crop yields using the Crop Growth Monitoring System*  
749 *and a weather generator*. *Agric. For. Meteorology*. 164: 96-111.
- 750 Valbuena, D., Bregt, A. K., MacAlpine, C. and Seabrook, L., 2010. An agent-based approach to  
751 explore the effect of voluntary mechanisms on land use change: a case in rural queensland,  
752 Australia. *Journal Of Environmental Management*, 91(12):2615-2625.
- 753 Verburg, P.H., Schot, P.P., Dijst, M.J. and Veldkamp, A., 2004. Land use change modelling: current  
754 practice and research priorities. *GeoJournal*. 61: 309-324.
- 755 Vidal, J-P., Martin, E., Franchistéguy, L., Baillon, M. and Soubeyroux, J.M., 2010. A 50-year high-  
756 resolution atmospheric reanalysis over France with the Safran system. *International Journal of*  
757 *Climatology*. 30(11): 1627-1644. DOI: 10.1002/joc.2003.10.1002/joc.2003. Meteo-00420845.
- 758 Warner, J.C., Perlin, N. and Skillingstad, E.D., 2008. Using the Model Coupling Toolkit to couple  
759 earth system models. *Environ. Modell. Software*. 23: 1240-1249.
- 760 Wolf, J. and van Diepen, C.A., 1995. Effects of climate change on grain maize yield potential in the  
761 European Community. *Clim. Change*. 29 (3): 299-331.
- 762 Zheng, G. and Moskal, L.M., 2009. Retrieving Leaf Area Index (LAI) Using Remote Sensing:  
763 Theories, Methods and Sensors. *Sensors*. 9: 2719-2745. doi.org/10.3390/s90402719
- 764 **Appendices**
- 765 Appendix A
- 766 Table A.1: Parameters used in the co-simulation approach.

Category	Name	Description	Unit	Value	
<i>Optirrig model</i>				<i>Winter cereal</i>	<i>Spring Cereal</i>
Plant	$a_w$	Controls the decrease of $H_i$ for low $LAI$ values	-	0.1	0.2
	$H_{i\ pot}$	Potential $H_i$ (Harvest Index)	-	0.5	
	$K_{c\ max}$	Maximum value of $K_c$ (crop coefficient)	-	1.2	
	$LAI_{max}$	Maximum $LAI$ value	-	6	7
	$G_{hu}$	Percentage of grain humidity	-	15	
	$RUE$	Radiation Use Efficiency	-	1	
	$\alpha\ 1$	First shape parameter for $LAI$ curves	-	2	20
	$\alpha\ 2$	Second shape parameter for $LAI$ curves	-	2	3.5
	$\beta$	Third shape parameter for $LAI$ curves	-	6	2.5
	$\lambda$	Harmfulness of the water stress	-	1.25	
Soil	$K_{ru}$	Easily usable reserve/field capacity	-	0.6	0.65
	$P_{max}$	Maximum profile and rooting depth	m	0.36	
	$\theta_{fc}$	Field capacity	-	0.29	
	$\theta_{wp}$	Wilting point	-	0.12	
Temperature	$T_i$	Temperature sum for root installation	°C	450	200
	$T_M$	Temperature sum to reach the maximum $LAI$	°C	1700	1200
	$T_s$	Temperature sum for crop emergence	°C	100	80
	$T_{s1}$	Temperature sum for the 1st critical stage	°C	900	
	$T_{s2}$	Temperature sum for the 2nd critical stage	°C	2100	1600
Management	-	Soil reserve when starting the simulation	mm	340	
	-	Sowing DOY	-	1	198
<i>WatASit model</i>					
	$K$	Maximum number of days since the last irrigation of the plot, or with precipitation inferior to $P$	-	12	



Irrigation decision-rules	<i>N</i>	Maximum number of days without irrigation, if this number is reached, irrigation shall be abandoned on that parcel for the remainder of the irrigation campaign	-	45
	<i>P</i>	Amount of precipitation receive during the last N days. Irrigation of the plot is considered only if this quantity is not reached.	mm	120
Irrigation operation	<i>D</i>	Target duration to flood a plot	h/ha	4
Gravity-fed network	<i>Qref</i>	The reference flow rate at the network intake	$m^3 s^{-1}$	0.09
	<i>DivCoeff</i>	The diversion coefficient at the network junctions	-	0.5
	<i>S</i>	The seepage rate considered along each network branch	$m^3 s^{-1} .km^{-1}$	0.0067
	<i>Qflood</i>	The minimum flow rate required to flood a farm plot served by the gravity-fed network	$m^3 s^{-1}$	0.03
	<i>Qrung</i>	The flow rate corresponding to a floodgate rung at the network intake. When agents ask for more water, flow at the network increases by this value, until overflow rate is reached.	$m^3 s^{-1}$	0.01
	<i>Qmax</i>	The overflow rate of the network : flow rate at the intake cannot exceed the value	$m^3 s^{-1}$	0.15
Irrigation dose	<i>Idose</i>	Fixed irrigation dose	mm	43.2
<i>Co-simulations</i>				
Start_simulation_date (DOY)	<i>startDate</i>	The date when simulation starts.	-	15/10/2016 (1)
Start_irrigation_date (DOY)	<i>irriDate</i>	The date when the irrigation campaign starts.	-	1/5/2017 (198)
End_simulation_and_irrigation_date (DOY)	<i>endDate</i>	The date when the irrigation campaign ends, and also the simulations.	-	31/7/2017 (289)